ANONLINEAR ANALYSIS OF FIBROUS REINFORCED CONCRETE SLABS BY ASSUMED STRAIN AND HETEROSIS ELEMENTS

Dr. A. A. Abdul-Razzak — Assist. Professor
Nuha H. Al-Jubory — Assist. lecturer
College of Engineering/ Mosul University, Mosul-Iraq

Abstract

In the present work, the finite element method has been used to investigate the behavior of fibre reinforced concrete slabs in the pre and post-cracking levels up to the ultimate load. Assumed transverse shear strain is used in the formulation to overcome the shear locking, and Heterosis elements are employed in the analysis.

Both an elastic-perfectly plastic and strain hardening plasticity approach have been employed to model the compressive behavior of the fibre concrete. The yield condition is formulated in terms of the first two stress invariants. Concrete crushing is a strain-controlled phenomenon, which is monitored by a fracture surface similar to the yield surface. A layered approach is adopted to discretize the concrete through the thickness. A tension stiffening model has been suggested by making a regression analysis of the experimental results, with index of determination (90.61%).

The steel is considered either as an elastic perfectly plastic material or as an elastic-plastic material with linear strain hardening. Steel reinforcement is assumed to have similar tensile and compressive stress-strain relationship.

Keywords: Finite Element Method, Slab, Steel Fibre Reinforced Concrete, Tension Stiffening Model.

ألتحليل غير الخطي_للبلاطات الخرسانية الليفية المسلحة بطريقة العناصر المحددة ذات الانفعال المفروض

د. أياد أمجد عبد الرزاق — أستاذ مساعد
نهى حميدي الجبوري — مدرس مساعد
كلية الهندسة / جامعة الموصل

الخلاصة

في هذا البحث تم إجراء التحليل غير الخطي بطريقة العناصر المحددة لبحث أداء البلاطات الخرسانية الليفية المسلحة في مرحلة ما قبل التشقق وبعدها إلى الحمل الأقصى. استخدم نوعين من العناصر ، العناصر ذات الانفعال المفروض للتخلص من ظاهرة القفل بالقص وعناصر هيتروسز .

مثل سلوك الخرسانة في حالة الانضغاط كمادة مرنة تامة اللدونة أو كمادة مرنة مع انفعالات لدنة متصلدة . شروط الخضوع عبر عنها بدلالة أول متغيرين للإجهاد . حركة سطوح التحميل المتعاقبة حكمت بقاعدة التصلب التي تحدد من علاقة الإجهاد – الانفعال أحادي المحور والمعبر عنها بدلالة قطع مكافئ . تهشم الخرسانة هي ظاهرة محكومة بالانفعال ومنظمة بسطح سحق يشبه سطح الخضوع . كما استخدم أسلوب تقسيم السمك إلى طبقات لتمثيل الخرسانة خلال السمك. ولغرض تمثيل تأثير صلابة الشد في الخرسانة المتشققة تم اقتراح نموذج بالاعتماد على نتائج عملية وقد أعطى هذا النموذج معامل توافق (90.61%). حديد التسليح اعتبر كمادة مرنة تامة اللدونة أو كمادة مرنة لدنة مع تصلب انفعال خطي.

Received 2/3/2009

Accepted 3/11/2009

NOTATIONS

d_f Equivalent diameter of fibre.
E_c Concrete elastic modulus.
E_{cf} Modulus of elasticity of SFRC.
E_i Initial modulus of elasticity of concrete.
E_s ,E_s' Initial and second modulus of elasticity for steel.
f_c' Uniaxial compressive strength of plain concrete.
f_{cf}' Uniaxial compressive strength of SFRC.
f_t' Uniaxial tensile strength of matrix.
f_{tf} Uniaxial tensile strength of composite.
f_u Average tensile stress of fibres crossing the cracked section.
G_f Fracture energy of SFRC.
l_f Length of fibre.
N_f *Effective number of fibres per unit cross section area*
V_f Volume fraction of fibre.
ε_1 ,ε_2 Strain in principal direction 1 and 2 respectively.
ε_{cuf} Ultimate crushing strain of SFRC.
ε_m Limiting tensile strain normal to the crack.
ε_{pf} Compressive strain at peak stress of SFRC.
ε_t Tensile strain at peak stress of matrix.
ε_{tf} Tensile strain at peak stress of composite.
σ_t Tensile stress
τ_u Average characteristic bond strength.
ν Poisson's ratio.

Introduction

The purpose of the present paper is to study the behavior of fiber reinforced concrete slabs by using heterosis elements [1] and assumed strain elements [2]. Heterosis elements are a 9-node quadrilateral, which employs serendipity shape function for the transverse displacement, and Lagrange shape function for the rotations.

To enhance the weak properties of concrete such as tensile strength and ductility, steel, glass, polymer and other types of fibres have been added as reinforcement, thus producing a composite material. The mechanical behavior of the resulting composite material is substantially different from that of the matrix material and possessing higher tensile strength, ductility and fracture toughness.

Huang [2] used an artificial method for the elimination of shear locking by interpolating new shear strain fields from the strain values at the sampling points which are appropriately located in individual elements.

The Behavior of Fibrous Concrete in Uniaxial Compression

The additional of fibre to the concrete increased the compressive strength and the peak strain as defined below [3]:

$$f_{cf}^{`} = f_c^{`} + 3.6\frac{V_f l_f}{d_f} \quad (1)$$

$$\varepsilon_{pf} = 0.0021 + 0.0007\frac{V_f l_f}{d_f} \quad (2)$$

where

$f_{cf}^{`}, f_c^{`}$ is the compression strength of standard cylinder for plain and fibre reinforced concrete in (MPa).

V_f is fibre percentage by volume.

l_f, d_f is fibre length and diameter.

The modulus of elasticity of fibre reinforced concrete calculated using the following equation [4]:

$$E_{cf} = 0.43 E_s V_f + E_c (1 - V_f) \quad (3)$$

E_s, E_c is modulus of elasticity of steel fibre and concrete respectively .

The ultimate strain in compression can be calculated using the following equation [5]:

$$\varepsilon_{cuf} = (3011 + 2295\, V_f) * 10^{-6} \quad (4)$$

The Behavior of Fibrous Concrete in Uniaxial Tension

a) The ascending part:

A simple expression that has been used for defining uniaxial tensile stress-strain curve up to the peak stress value of plain concrete[6]. This model is used by taking the effect of fibre reinforced concrete parameters [7], the comparison between experimental [8] and numerical model shown in Fig.(1):

$$\sigma_t = f_{tf}\left[1 - \left(1 - \frac{\varepsilon}{\varepsilon_{tf}}\right)^A\right] \quad (5)$$

f_{tf} : tensile stress at tensile strain ε_{tf}

$$f_{tf} = f_t^{'}(1 + 0.016 N_f^{1/3} + 0.05\pi\ d_f l_f N_f) \quad (6)$$

Where:

N_f is the number of fibres crossing a unit area

$$N_f = 1.64\ V_f / \pi d_f^2 \quad (7)$$

$$A = E_i \frac{\varepsilon_{tf}}{f_{tf}} \quad (8)$$

(E_i): initial tangent modulus.

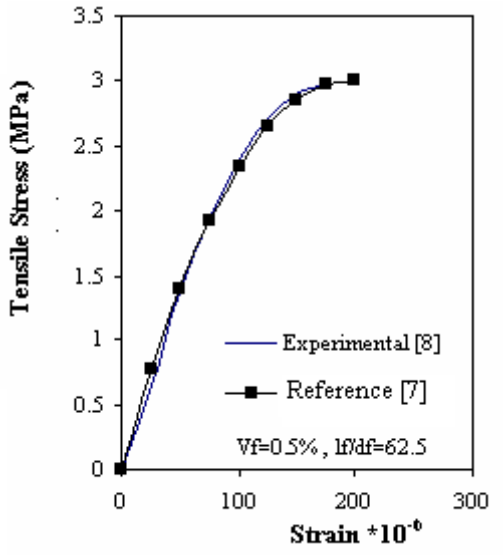

Fig.(1) The ascending part of tension

b) The descending part:

By making regression analysis of the experimental results of references [9 and 10], the following model is adopted to express the relationship between post-peak stress and strain [7], the comparison between experimental and numerical model shown in Fig.(2), (with index of determination=90.61%):

$$\sigma_t = f_{tf} e^{-f_{tf} S\left(\frac{\varepsilon}{\varepsilon_{tf}} - 1\right)^R} \quad (9)$$

Where S and R : constants depend on fibre volume fraction V_f and aspect ratio $\frac{l_f}{d_f}$.

$$S = 0.66875 - 0.48842\left(V_f \frac{l_f}{d_f}\right) + 0.1125\left(V_f \frac{l_f}{d_f}\right)^2 \quad (10)$$

$$R = 6.26513\left(\frac{l_f}{V_f . d_f}\right)^{-0.50327} \quad (11)$$

After crack happened the elastic modulus and Poisson's ratio are reduced to zero in the direction perpendicular to the crack and a reduced shear modulus is employed to simulate aggregate interlock. Two different approaches are used to reduce the shear modulus:

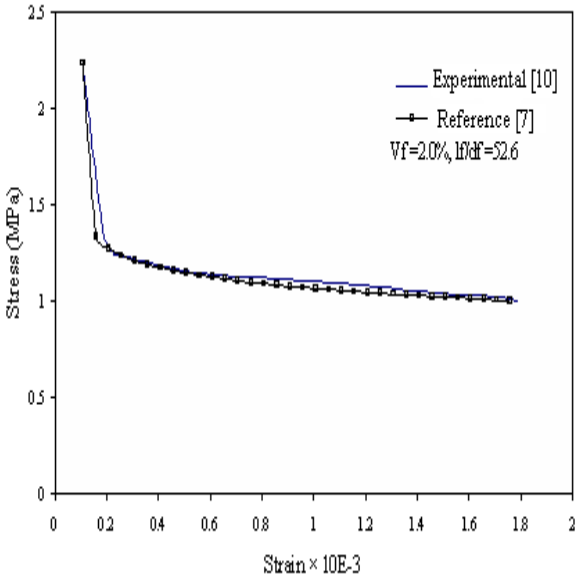

Fig.(2) The descending part of tension model

(i) Approach named G1: This approach was proposed initially by Al-Mahaidi [11]. and modified by many investigations [5,12 and 13] by substituting ε_{tf} for ε_t. The shear modulus of cracked concrete G can be calculated as follows:

$$G` = \frac{0.4G}{(\varepsilon_1 / \varepsilon_t)} \quad (12)$$

(ii) Approach named G2: This approach was proposed initially by Abdul-Razzak [5]. According to this approach, for concrete cracked in direction 1:

$$G`_{12} = 0.25G\left[\frac{\varepsilon_1 - \varepsilon_m}{\varepsilon_{tf} - \varepsilon_m}\right]^2 \quad \text{for} \quad \varepsilon_1 < \varepsilon_m$$

$$G`_{12} = 0 \quad \text{for} \quad \varepsilon_1 > \varepsilon_m \quad (13)$$

Where:

$$\varepsilon_m = \frac{3G_f}{h.f_u} + \varepsilon_{tf} \quad (14)$$

$$G_f = 0.04592\frac{V_f l_f^2}{d_f} \quad (15)$$

$$f_u = 0.41 V_f \tau_u l_f / d_f \quad (16)$$

$$\tau_u = 2.62 - 0.0036 N_f \quad (17)$$

Numerical Application

Example 1.

A simply supported square slab was tested by Ali [14]. The test specimen has (1800*1800)mm with (125)mm thickness and an effective depth of (100)mm to steel reinforcement. The material properties of tested slab are summarized in Table(1). The slab was modeled by four elements. Due to the symmetry of the slab, only are quarter of the slab is analyzed. Four steel layers are used to represent the reinforcement and eight concrete layers are found to be enough for the analysis. All dimension and detail of the slab shown in Fig.(3).

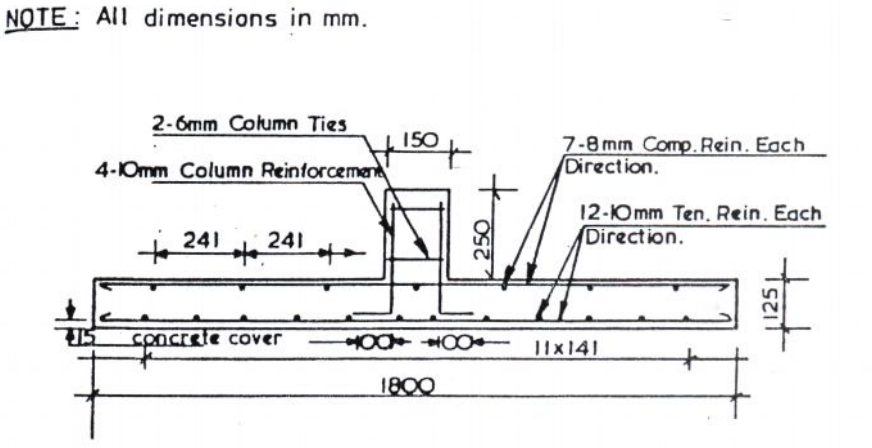

Fig.(3) Dimension and detail of slab No.(S-2) [14]

Table (1) Details of the slab of reference [14].

Slab No.	E_{cf} MPa	E_s MPa	V_f^* %	f'_{cf} MPa	f_{tf} MPa	f_y MPa	$\frac{l_f}{d_f}$	As` Bar	As Bar	ε_{cuf}
S-2	35480	204000	0.6	34.8	3.44	460	100	7-Φ8	12-Φ10	0.0044

ν_c =0.15 .

* Crimped steel fibre 0.5*50 mm

Fig. (4) shows a comparison between two models of cracked shear modulus G1 and G2. These two models give good agreement compared with experimental results. However, G1 model give ultimate load less than G2 model for both the assumed and heterosis elements. Both of G models give ductile results compared to experimental results.

Fig.(5) shows a comparison between the assumed strain element and 9-node Lagrangian degenerate element. The used of 9-node Lagrangian degenerate element shows stiff results and larger failure loads, this may be due to the shear locking that happened in 9-node Lagrangian degenerate element.

Fig.(6) shows a comparison between the assumed strain element and heterosis element. Both elements show a good agreement compared with experimental results.

Fig.(7) shows the cross section of the slab (S-2), it is seen the cracks that happened in the slab at the ultimate load, and the yield of concrete under the load.

Fig.(8) shows crack patterns at 84kN, 156kN, 192kN and at ultimate load using G2 model, it is seen that the cracks increased when the load increased.

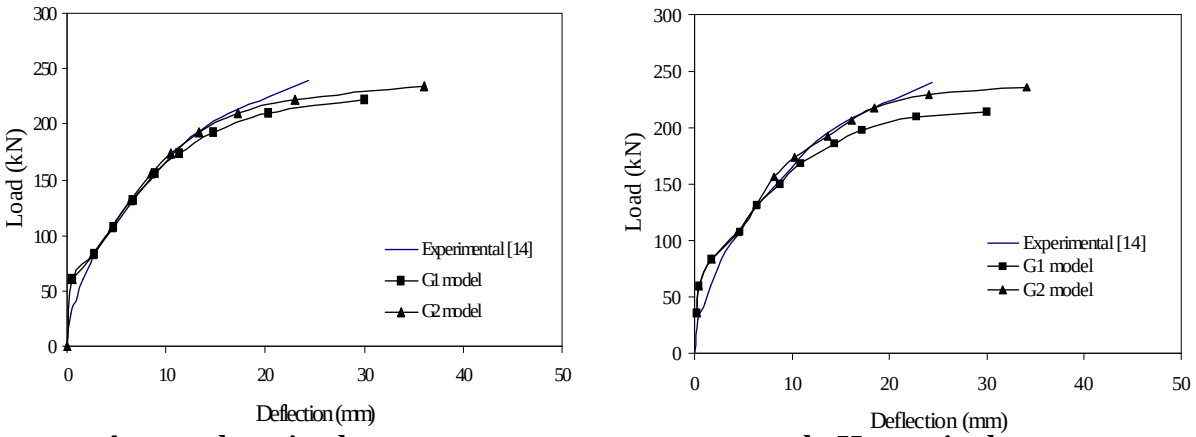

a. Assumed strain elements **b. Heterosis elements**

Fig.(4) The effect of G1 and G2 models on load deflection curves.

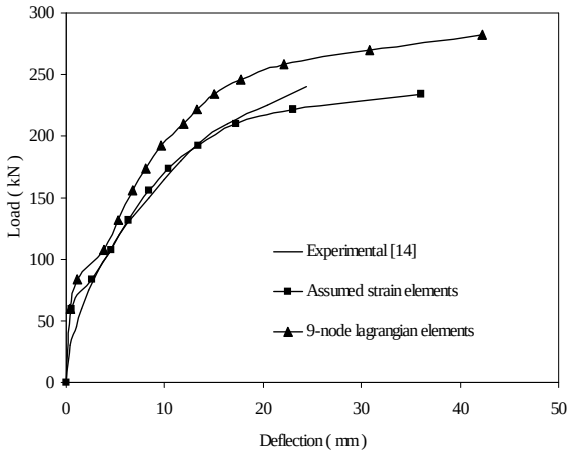

Fig.(5) The comparison between assumed and lagrangian element on load deflection curves.

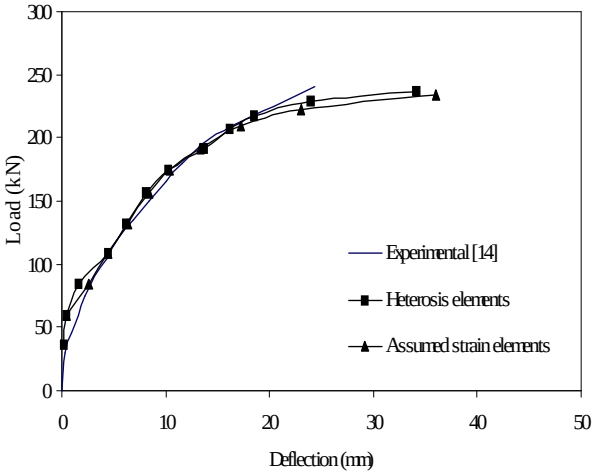

Fig.(6) The comparison between assumed strain and heterosis elements on load deflection curves.

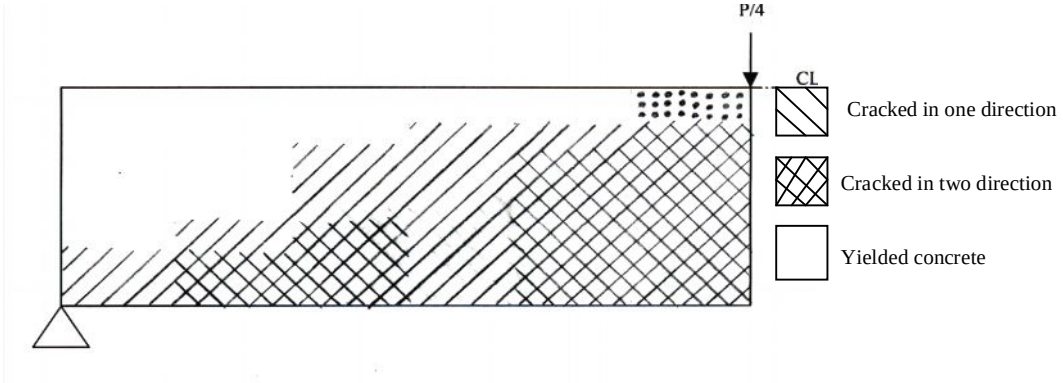

Fig.(7) Cross section of slab (S-2) at ultimate load

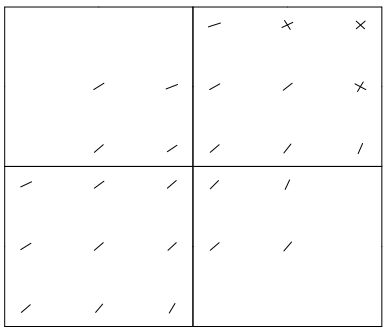

a) At load 84kN

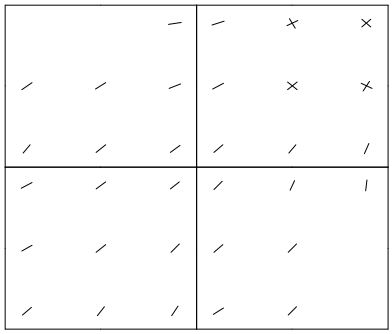

b) At load 156kN

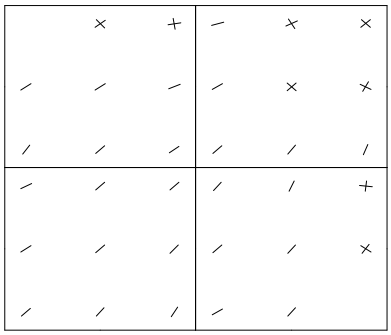

c) At load 192kN

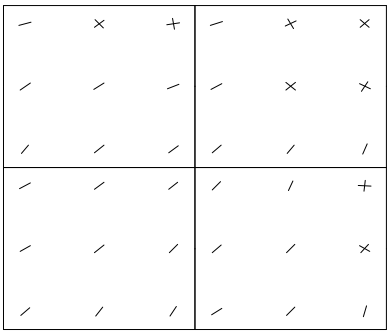

d) At ultimate load

Fig.(8) Crack pattern of slab (S-2)

Example 2.

A simply supporting circular slab was tested by Walraven J. et al [15]. The diameter of slab was (1750) mm and the total depth was (140) mm, and the effective depth of (110) mm to steel reinforcement. The material properties of the tested slab are summarized in Table (2). The slab is modeled by three elements. Due to the symmetry of the slab, only are quarter of the slab is analyzed. Two steel layers are used to represent the reinforcement and eight concrete layers are found to be enough for the analysis. All dimensions and details of the slab shown in Fig.(9), and finite element mesh shown in Fig.(10).

Table (2) Details of the slab of reference [15].

Slab No.	E_{cf} MPa	E_s MPa	V_f^* %	f'_{cf} MPa	f_{tf} MPa	f_y Mpa	$\frac{l_f}{d_f}$	ρ %	ε_{cuf}
S-6	29317	200000	1.0	38.8	3.5	465	62.5	1.0	0.0053

ν_c =0.15 .

*Paddled steel fibre 0.8*50 mm

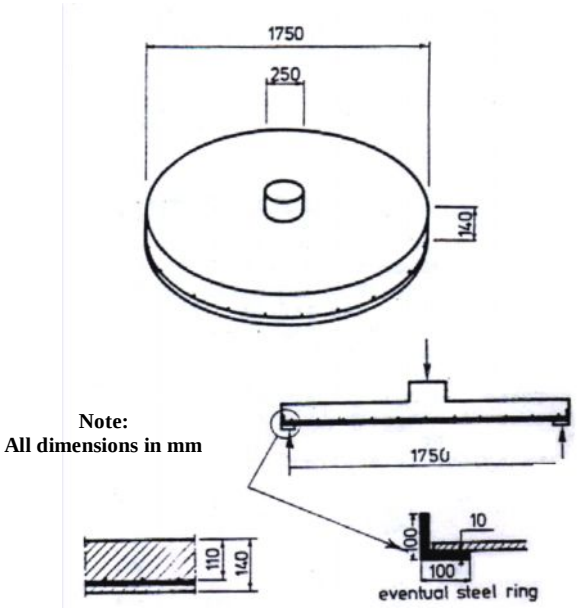

Fig. (9) Dimensions and details of slab No.(S-6)

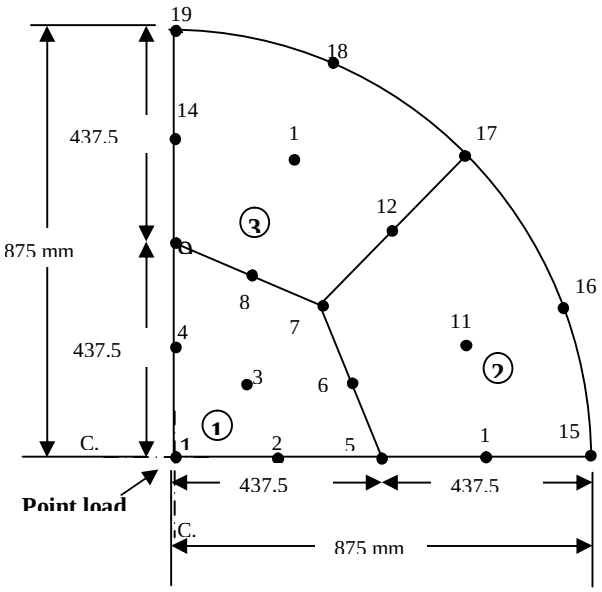

Fig. (10) Finite Element Mesh of (S-6)

Fig. (11) shows a comparison between two models of cracked shear modulus G1 and G2. These two models give small softening when compared with experimental results. However, G2 gives results of ultimate load more than G1 model.

Fig.(12) shows a comparison between the used of assume strain elements and heterosis elements. The used of two elements show a good agreement with experimental results.

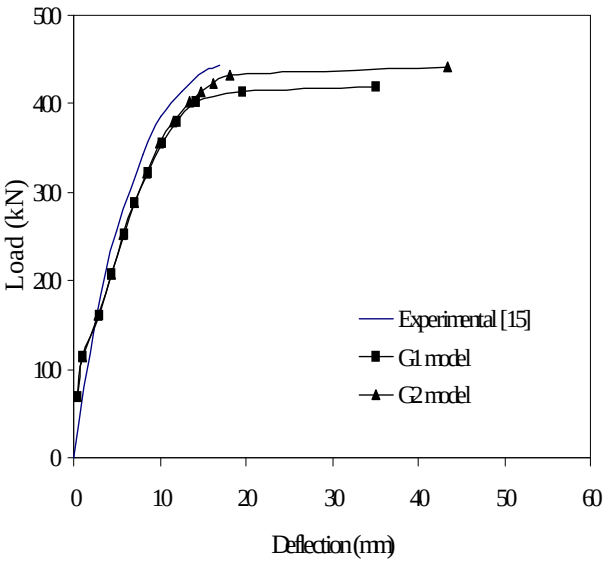

a. Assume strain elements

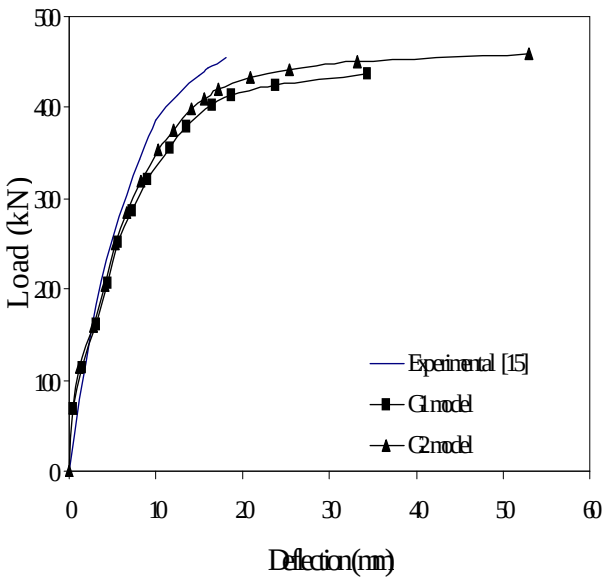

b. Heterosis elements curves.

Fig.(11) The effect of G1 and G2 model on load deflection

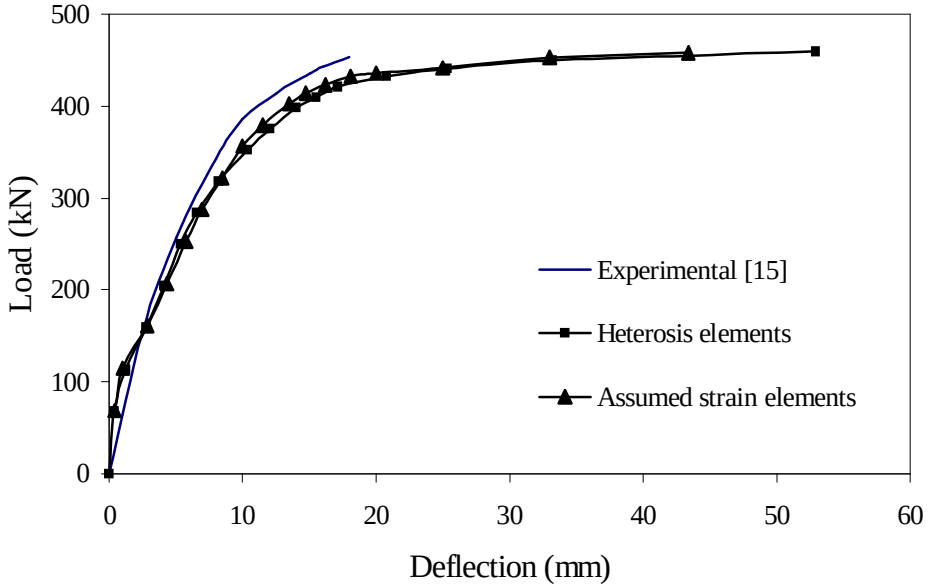

Fig.(12) The comparison between Assume strain and Heterosis element on load deflection curves.

Conclusions

1. The developed models for fiber concrete concerning the strain hardening plasticity and tension stiffening models proved to give satisfactory results for the analysis of reinforced concrete slabs subjected to incremental loading up to failure.
2. Two shear moduli of cracked fibre concrete is used and it is concluded that the shear crack approach G2 gives better results than G1 approach compared to experimental results.
3. The assumed strain and heterosis elements proved to be efficient for nonlinear analysis of fibrous reinforced concrete slabs, and no locking was detected in these types of elements.

References

1. Hughes, T.J.R., and Cohen, M., " The heterosis finite element for plate bending ", J. of Computers and Structures Vol. 9, 1978, pp. 445 – 480.
2. Huang, H.C., "Static and Dynamic Analysis of Plates and Shells theory, Software and Applications", Springer, Verlag, Berlin, Heidelberg 1989.
3. Soroushian, P., and Lee, C. D., "Constitutive modelling of steel fiber reinforced concrete under direct tension and compression", Proc. of the Inter. conf. on recent developments in fiber reinforced cements and concrete, 18-20 Sept. 1989, Cardiff (U.K.), Eds. Swamy and Barr, Elsevier Applied Science, pp. 363-377.
4. Patton, M.E., and Whittoker, W.L., " Effects of fiber content and damaging load on steel fiber reinforced concrete stiffness ", ACI J., Vol. 80, No. 2, January – February 1983, pp. 13 – 16.
5. Abdul-Razzak, A.A., " Nonlinear finite element analysis of fibrous reinforced concrete structural members " Ph.D. Thesis, University of Mosul, Iraq, Aug. 1996, 233 pps.
6. Gopalaratnam, V.S., and Shah, S.P., " Softening response of plain concrete in direct tension ", ACI J., Vol. 82, No. 27, May – June 1985, pp. 310 – 323.

7. نهى حميدي الجبوري,"التحليل غير الخطي بطريقة العناصر المحددة للبلاطات الخرسانية الليفية المسلحة. اطروحة ماجستير, جامعة الموصل , تشرين الثاني 2002.
8. Shah, S.P., and Gopalatnam, V.S., " Micromechanical and model for the tensile fracture of stell fibre reinforced concrete ", in RILEM Symp. on Developments in fiber Reinforced Cement and Concrete (Eds. R.N. Swamy, and R.L. Wagstaffe and D.R. Sakley), University of Sheffield Press, 13 – 17 July 1986, Sheffield, pp. 17 – 26 .
9. Mansur, M.A., Nagataki, S., Lee, S.H., and Oosumimoto, Y., " Torsional response of reinforced fibrous concrete beams ", ACI Structural Journal, Vol. 86, No. 1, Jan – Feb 1989, pp. 36 – 44.
10. Lim, T.Y., Paramasivam, P., Mansur, M.A., and Lee, S.L.," Tensile behaviour of steel `fibre reinforced concrete composites ", Proceedings, 3rd RILEM International Symposium on Developments in fibre Reinforced Cement and Concrete, University of Sheffieid Press, 13-17 July 1986, Sheffield, pp. 7 – 15.
11. Al-Mahaidi, R.S.H., " Nonlinear finite element analysis of reinforced concrete deep members ", Ph.D. Thesis, Dept. of Structural Engineering, Cornell University, Ithaca, New York, May 1978, 374 pps.
12. Al-Ta'an, S.A. and Abdul-Razzak, A.A., "Nonlinear finite element analysis of fibrous reinforced concrete corbels", AL-Rafidain Engineering Journal, Vol. 11, No. 1, 2003, pp. 34-46.
13. Abdul-Razzak, A.A. and Al-Ta'an, S.A., "Nonlinear finite element analysis of fibrous reinforced concrete deep beams", AL-Rafidain Engineering Journal, Vol. 11, No. 1, 2003, pp. 47-62.
14. Ali, S.A.R., "Effect of fiber reinforcement on the punching shear of flat plates", Ph.D. Thesis, University of Sheffield, UK, April 1979, 241 pps.
15. Walraven, J., Pat, T., and Markor, I., "The punching shear resistance of fibre reinforced concrete slabs", in RILEM Symp. on Developments in Fiber Reinforced Cement and Concrete (Eds. R.N. Swamy, R.L. Wagstaffe and D.R. Sakley), University of Sheffield Press 13 – 17 July 1986, Sheffield, pp. 569 – 577.

The work was carried out at the University of Mosul